



# Journal of Applied Sciences

ISSN 1812-5654

**science**  
alert

**ANSI***net*  
an open access publisher  
<http://ansinet.com>

## Estimation of Fault Location on a Radial Distribution Network Using Fault Generated Travelling Waves Signals

<sup>1</sup>Hashim Hizam and <sup>2</sup>P.A. Crossley

<sup>1</sup>Department of Electrical and Electronic Engineering, Faculty of Engineering,  
Universiti Putra Malaysia, 43400, UPM Serdang, Selangor, Malaysia

<sup>2</sup>School of Electrical and Electronic Engineering, Queen's University Belfast, Ashby Building,  
Stranmillis Road Belfast BT9 5AH, Northern Ireland

---

**Abstract:** This study describes a technique to estimate the location of faults on a radial distribution network based on the principles of travelling waves. The occurrence of faults on power systems will result in the high frequency voltage and current signals to propagate along the power systems. These signals contain a lot of information and can be used for fault location. Using the travelling wave technique, the high frequency components are extracted at one measurement point and analysis of the extracted signals is done by comparing the relative distance of each peak in the signals to the known reflection points in the distribution network. From this analysis identification of the fault section and the probable location of the fault can be made by tracing the paths of the high frequency signals generated from the faults. The power system simulator, PSCAD/EMTDC is used to model the distribution network and faults at various locations are simulated. The resulting simulated current waveforms are then cross-correlated against the original signal. A high cross-correlation value will indicate that the signals have a high degree of similarity with the original signal and indicate the most likely location of the faults. One significant finding from this work is that the faulty section of the distribution network can be determined accurately using information from only one end and hence it would be economical to be implemented as only one travelling wave fault locator is required, whereas in most of the travelling wave methods, the locations of the faults are located based on a double ended technique and are on transmission networks.

**Key words:** Fault location, travelling waves, cross-correlation, distribution network, single-ended

---

### INTRODUCTION

One of the main objectives of an electricity provider is to ensure reliable and continuous supply to its customers. If a fault occurs on power systems, protection schemes are expected to operate and clear the fault by opening the circuit breakers and disconnect the faulted line. If the fault is successfully cleared, an auto recloser scheme is used to restore the line. However, if the reclosing attempts are not successful, the circuit breaker will remain open and the fault can be categorised as a permanent fault (Glover and Sarma, 2001). Under this condition it is necessary to send a repair crew to the point of fault, repair the damage and restore the line back into operation. For efficient despatch of the repair crew, it is essential that the fault location can be determined accurately and rapidly. High fault location accuracy will help speed up the repair process as the repair crew will only need to inspect a short section of the faulted line.

Fast restoration of the affected line will certainly benefit both the service provider and the customers.

Fault detection and location based on the fault induced current or voltage travelling waves has been studied for many years (Ancell and Pahalawaththa, 1994; Bo *et al.*, 1999; Crossley and MacLaren, 1983; Crossley *et al.*, 2001; Elhaffar and Lehtonen, 2004; Evrenosoglu and Abur, 2005; Jie Liang *et al.*, 1999; Thomas *et al.*, 2004; Xiangjun *et al.*, 2004). In all these techniques, the location of the fault is determined using the high frequency transients instead of the steady state components. The main idea behind these techniques is based on the reverberation of the fault generated travelling waves in the faulty system. With GPS technology, the travelling waves based technique can provide a fault location accuracy of a few hundred meters (Gale and Giannattasio, 1994).

Fault location based on the travelling waves can generally be categorised into two techniques,

single-ended and double-ended. For single-ended, the current or voltage signals are measured at one end of the line and fault location relies on the analysis of these signals to detect the reflections that occur between the measuring point and the fault. For the double-ended method, the time of arrival of the first fault generated signals are measured at both ends of the lines using synchronised timers. The double-ended method does not require multiple reflections of the signals. However, single-ended location is preferred as it only requires one unit per line and a communication link is not necessary. Thus for distribution systems, if this method can be shown to be reliable, it should be less expensive and therefore preferable. This is the basis of the research work presented in this study.

**Travelling waves fault location: Theory and principle:**

Travelling waves on power systems can be caused by many factors such as faults, lightning and switching activities. On overhead lines the waves travel at a speed close to the speed of light i.e., 300000 km sec<sup>-1</sup> and are detected as a voltage and a current wave.

The voltage and current on a loss-less uniform power line are related by the telegraphy equations (Bewley, 1951).

$$\frac{\partial v(x,t)}{\partial x} = -L \frac{\partial i(x,t)}{\partial t} \tag{1}$$

$$\frac{\partial i(x,t)}{\partial x} = -C \frac{\partial v(x,t)}{\partial t} \tag{2}$$

C and L are the capacitance and inductance of the lines per metre whereas v(x,t) and i(x,t) are the voltage and current changes at location x at time t due to the travelling wave. The solutions to the above equations are:

$$v(x,t) = f_1(t - x/c) + f_2(t + x/c) \tag{3}$$

$$i(x,t) = \frac{1}{Z_0} f_1(t - x/c) - \frac{1}{Z_0} f_2(t + x/c) \tag{4}$$

Where, c is velocity of the wave propagation and Z<sub>0</sub> (Z<sub>0</sub> = √L/C) is the characteristic impedance of the lines. The functions f<sub>1</sub> and f<sub>2</sub> are arbitrary functions which represent two waves which travel in opposite directions.

When a fault occurs on a power line, the voltage and current will experience a sudden change in value. This abrupt change will initiate a wave which propagates away from the fault towards both ends of the line. At a discontinuity such as a busbar, a junction, a short circuit or an open circuit, this wave will be both reflected and

transmitted. This wave will then continue to be reflected and transmitted until it dies out due to attenuation.

The basic principle of most single-ended travelling wave fault locators is to evaluate the fault location using the time interval between the arrival of an incident travelling wave generated by a fault and the corresponding wave reflected from the fault point (Crossley and MacLaren, 1983; Crossley *et al.*, 2001; Jie Liang *et al.*, 1999). However, since travelling waves can also be reflected by other discontinuities, identification of the desired signal is of crucial importance to the accuracy of the location decision. The most widely used analysis method is based on cross-correlation; the incident travelling wave is taken as a reference and the signal that contains the subsequent backward travelling waves is cross-correlated with the reference. The basic idea is that the desired backward travelling waves has the same shape as the reference and generates a peak in the correlation output.

Existing travelling wave based fault locators have been applied mostly to transmission lines rather than on distribution lines. This is because distribution lines are comparatively short in length and hence it is difficult to detect separately the arrival of a fault generated incident wave and the arrival of the subsequent backward travelling waves. Moreover, a distribution line generally contains many branches which would cause multiple reflections and reduce the magnitude of the travelling waves as they propagate along the line. These branches complicate the process of identifying the desired signal.

A Bewley Lattice diagram shown in Fig. 1 can be used to describe the reverberation of a travelling wave in a power system.

If the time interval between the arrival of the incident wave at A1 and that of the reflected wave at A4 (Fig. 1) is obtained, the distance to the fault from A can be calculated as:

$$d = ct/2 \tag{5}$$

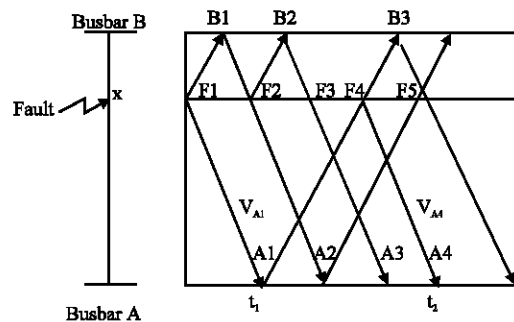


Fig. 1: Bewley Lattice diagram

Where:

- c = The travelling wave velocity
- t = The time interval ( $t = t_2 - t_1$ )

In this study, the paths of the travelling waves will be traced based on the principles explained and the fault location is estimated by comparing the paths of the travelling waves and the known discontinuity points along the network.

**MATERIALS AND METHODS**

A 33/11 kV distribution was modelled using PSCAD/EMTDC. A single line diagram of the distribution feeder is shown in Fig. 2. The network consists of a short section of underground cable (section A-AA) supplying an overhead line. The total distance of the main feeder (A-A1) is 14.98 km and the cable section is 1.5 km. The conductor parameters for the overhead lines were as follows:

- No. of conductors: 3
- Conductor radius: 0.005025 m
- Conductor DC resistance: 0.5426 ohm km<sup>-1</sup>
- Height of conductors above the ground: 6 m
- Horizontal spacing between phases: 0.8 m
- Ground wires: none
- Ground resistivity: 100 ohm m

The characteristic impedance of the overhead line is 348 Ω and the velocity of the travelling wave is almost 3×10<sup>5</sup> km sec<sup>-1</sup>, i.e., the speed of light.

The parameters for the cable result in a characteristic impedance of 39.7 Ω and a propagation velocity of 1.66×10<sup>5</sup> km sec<sup>-1</sup>, i.e., about 55.2% of the travelling wave velocity in free space.

Single phase to earth faults were simulated at various points along the main feeder and the current measurements were taken at point A. The fault resistance was set at 0.01 Ω and the time step for the simulation was 0.8 μ sec.

The proposed methodology of locating the fault as are follows:

- The high frequency components of the currents are measured at one end of the network, i.e., at A.
- Taking the first peak as the reference incident signal, the time delays between the subsequent peaks and the first peak are measured.
- From these time delays, the corresponding distances are calculated. These distances represent the travel paths of the signals in the network.
- Comparisons between the calculated distances and the known discontinuity points in the network are made. From this analysis, the faulty section can be identified.

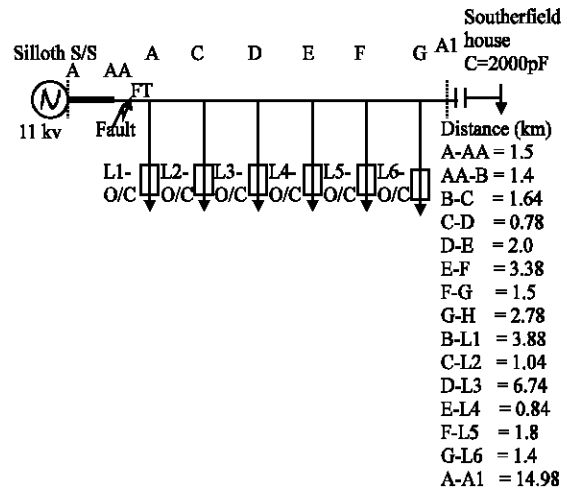


Fig. 2: Single line diagram of the distribution network

- Once the faulty section is identified, simulations can be made along the faulty section and the results compared using cross-correlation technique to find the most probable location of the fault.

**RESULTS AND DISCUSSION**

The current waveform (only the faulted waveform is shown) when a Phase A to earth fault with a 0.01 Ω fault resistance was simulated at a distance of 2.5 km from the measurement point A (the fault is between measurement point A and the first branch, B) (Fig. 3).

Since the network consists of underground cable and overhead line, the velocity of the travelling wave initiated by the fault will be different in the cable section and on overhead line. To avoid confusion, only the propagation speed on overhead line is used in the analysis. For correct analysis, the effective length of the cable section has to be calculated. In this case, the effective length of the cable section is 2.71 km instead of the actual length of 1.5 km. The effective fault distance to point A is then calculated to be 3.71 km.

Several peaks are identified and labelled as in Fig. 3. P1 is always known as it is the first incident fault surge and the subsequent peaks or surges come from reflection points that exist between the fault point and point A. If the time difference between P1 and the subsequent peak is obtained and using equation 5, the distance can be calculated. Table 1 shows the calculated distances of each peak relative to P1.

From Fig. 3, there are some peaks (P4 and 5) which are opposite in polarity compared to the incident fault surge, P1. Since the impedance of the cable is much lower than that of the overhead line, a positive incident current wave

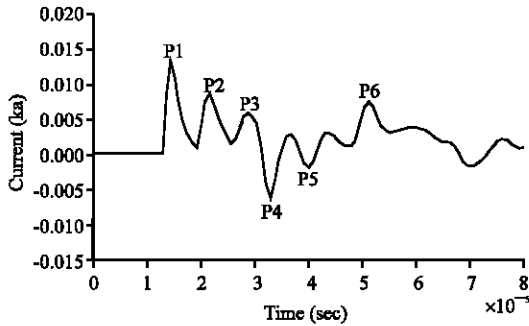


Fig. 3: Current waveforms for a fault at a distance of 2.5 km

Table 1: Calculated distance of each peak relative to P1 for fault at 2.5 km

Peak	Time delay ( $\mu$ sec)	Distance (km)
P1	0.0	0.00
P2	7.2	1.08
P3	14.4	2.16
P4	18.4	2.76
P5	25.6	3.84
P6	36.8	5.52

will be reflected with a negative polarity at a transition point between the cable section and overhead line. Therefore it can be assumed that the fault is located beyond the cable section (point AA). The calculated distance of P4 with respect to P1 confirms this, i.e., it is close to the effective length of the cable. As for P2, the calculated distance is the distance between the fault point and point AA (actual distance is 1.0 km). Comparing the calculated distances with the known distances in the network, the following assumptions can be made:

- P2 might be a surge reflected from L2 since the distance is close to the length of branch C-L2 (1.04 km).
- P4 corresponds to the surge reflected from point AA.
- P5 might be a surge reflected from L1 since the distance is close to the length of branch B-L1 (3.88 km).

From the assumptions, it might seem that the fault could be beyond point C since there are reflections from L1 and L2. However, analysis on the polarity of the surge suggests that P5 could not be the surge reflected from L1 as the surge reflected from that point is expected to be positive in polarity. Taking that into consideration, the fault is now assumed to be between point AA and B. P2 is therefore the surge reflected from the fault point.

For a fault distance of 3.4 km, i.e., between point B and C, the current waveform is described in (Fig. 4).

With reference to the waveform of Fig. 4, the time delay and the corresponding distances from P1 to each subsequent peak are shown in Table 2.

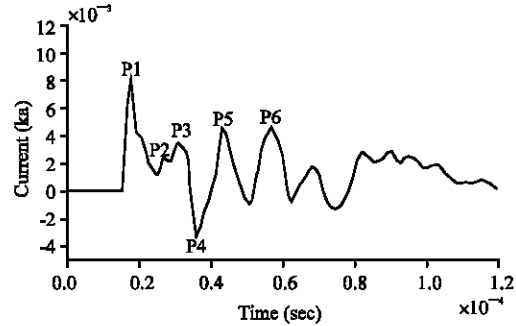


Fig. 4: Phase A current waveform for a fault at a distance of 3.4 km

Table 2: Calculated distance of each peak relative to P1 for fault at 3.4 km

Peak	Time delay ( $\mu$ sec)	Distance (km)
P1	0.0	0.00
P2	9.6	1.44
P3	13.6	2.04
P4	18.4	2.76
P5	25.6	3.84
P6	39.2	5.88

Comparing the calculated distance with the known distances in the network the following conclusions can be made:

- P2 corresponds to the surge reflected from point B (the distance from AA-B is 1.4 km).
- P4 corresponds to the incident surge reflected from the end of the cable.
- P5 is the surge reflected from the end of the branch L1 (the distance of branch B-L1 is 3.88 km).

From the above analysis, the location of the fault can be assumed to be beyond point B as there is a surge reflected from the end of the branch L1. Yet, the fault position cannot be beyond point C as there is no other peak that corresponds to any other length of a branch beyond C. Since the length of the section from point B and C is 1.64 km, the estimated fault location is between 2.9 and 4.54 km from A.

For a fault distance of 4.94 km, i.e., between point C and D, the current waveform is shown in Fig. 5.

The time delay between the P1 and the subsequent peaks are measured and the corresponding distances are calculated as shown in Table 3.

Comparing the calculated distance with the known distances in the network the following conclusions can be made:

- P2 corresponds to the surge reflected from the end of the branch L2 (C-L2 = 1.04 km).

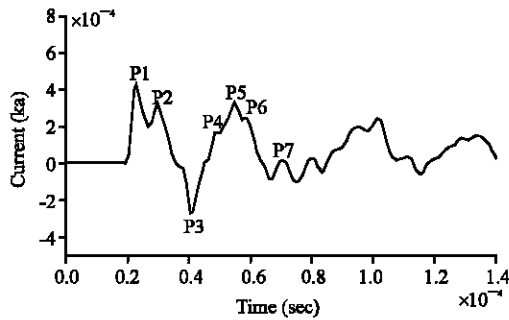


Fig. 5: Phase A current waveform for a fault at 4.94 km

Table 3: Calculated distance of each peak relative to P1 for fault at 4.94 km

Peak	Time delay ( $\mu$ sec)	Distance (km)
P1	0.0	0.00
P2	6.4	0.96
P3	18.4	2.76
P4	25.6	3.84
P5	32.5	4.80
P6	36.0	5.40
P7	48.0	7.20

- P3 corresponds to the incident surge reflected from the end of the cable.
- P4 is the surge reflected from the end of the branch L1 (B-L1 = 3.88 km).

Since there are reflections from L1 and L2 and none from the other known reflection points, the location of the fault can be identified to be in section C-D, i.e., the estimated fault location is between 4.54 and 5.32 km from A.

If the fault was simulated further away from the measurement point, the waveform become more complex due to multiple reflection points that exist between the fault and the measurement point. Fig. 6 shows the waveform when the fault is at 10.32 km from A.

The time delay and the corresponding distances from P1 to each subsequent peak are shown in Table 4.

Comparing the calculated distance with the known distances in the network the following conclusions can be made:

- P2 corresponds to a distance of 1.08 km, which is close to a known distance of branch C-L2 (1.04 km).
- P3, which corresponds to a distance of 2.88 km, can be assumed to be a surge reflected from either point B (the distance from A to B is 2.9 km) or point L4 (the length of branch E-L4 is 2.84 km) or a combination of both.
- P4 is the surge reflected from point L1 as the calculated distance is close to the length of branch B-L1 (3.88 km).

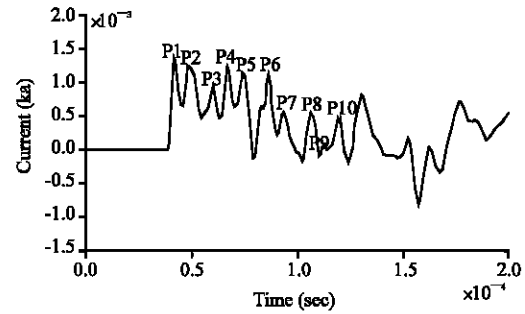


Fig. 6: Phase A current waveform for a fault at a distance of 10.32 km

Table 4: Calculated distance of each peak relative to P1 for fault at 10.32 km

Peak	Time delay ( $\mu$ sec)	Distance (km)
P1	0.0	0.00
P2	7.2	1.08
P3	19.2	2.88
P4	26.4	3.96
P5	32.8	4.92
P6	45.6	6.84
P7	52.8	7.92
P8	65.6	9.84
P9	72.0	10.80
P10	78.4	11.76

- P6 is the surge reflected from L3 as the calculated distance is close to the length of branch D-L3 (6.74 km).

Since there are reflection from L1, L2, L3 and L4, the faulty section can be identified as point E-F. Knowing the faulty section, the distance to the fault can be estimated to be between 7.32 to 10.70 km.

From all the analysis done, it can be said that the travelling wave principles can be used in order to trace the paths of the faulted signals and one significant finding that could be deduced is that the faulty section could be identified as the section beyond the last feeder whose peak appeared in the high frequency waveform.

**Cross-correlation analysis:** Since the surge impedance difference between the cable and overhead line is large (at point AA), the reflection factor at this particular point is also large. Therefore, if the fault is located beyond this point, only a small fraction of the incident fault surge reflected from the substation (point A) will return to the fault point. In this case, fault location estimation based on measuring the time delay between the arrival of the fault incident surge and the surge reflected from the fault will not be correct. However, since the fault section can be identified, faults can be simulated at several positions within the faulted section and the simulated waveforms can be cross-correlated against the original waveform.

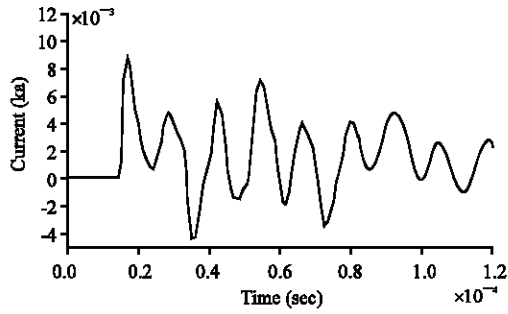


Fig. 7: Fault at 3.0 km

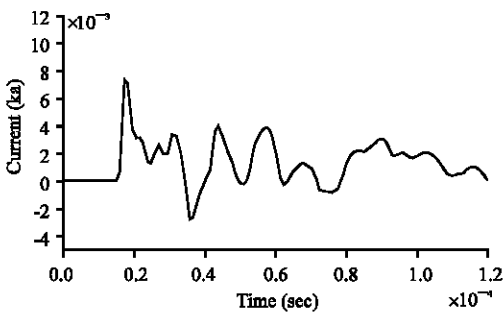


Fig. 8: Fault at 3.5 km

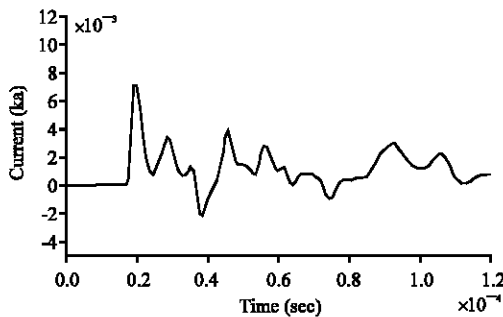


Fig. 9: Fault at 4.0 km

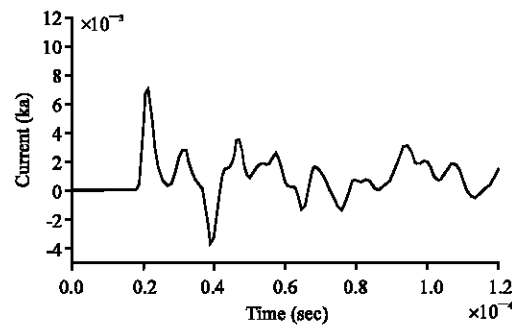


Fig. 10: Fault at 4.5 km

For case 2, the identified fault section is B-C and the fault can be anywhere from 2.90 to 4.54 km (Table 5).

Table 5: Summary of the fault section identification for all four cases

Case	Actual fault location	Identified fault section	Estimated fault location (km)
1	2.50	AA-B	1.50-2.90
2	3.40	B-C	2.90-4.54
3	4.94	C-D	4.54-5.32
4	10.32	E-F	7.32-10.70

Table 6: Correlation coefficient for probable fault distances for the fault at 3.4 km

Fault distance (km)	Cross-correlation window			Average
	Correlation coefficient (CC)			
3.0	50.00	75.00	100.00	0.9339
	0.9526	0.9309	0.9182	
3.5	50.00	75.00	100.00	0.9715
	0.9705	0.9718	0.9722	
4.0	50.00	75.00	100.00	0.8235
	0.8501	0.8180	0.8025	
4.5	50.00	75.00	100.00	0.7564
	0.8092	0.7491	0.7109	

Faults were simulated at 3.0, 3.5, 4.0 and 4.5 km from A and the waveforms were compared against the original waveform. Figure 7-10 show the simulated waveforms at these locations.

Visual inspection suggests that the waveform for a fault at 3.5 km (Fig. 8) is the closest match to the actual fault signal, shown in Fig. 4. In order to confirm this, a cross-correlation coefficient is calculated and the results are presented in Table 6.

The results confirm that the waveform for fault at 3.5 km is the closest match to the waveform of the original fault which was located at 3.4 km. The accuracy could be further improved if more waveforms matching were done around the location of the fault.

### CONCLUSIONS

This study presented a method based on high frequency travelling waves generated by the faults for fault location. The study based on simulations suggests that by calculating the relative distance of the peak in the high frequency travelling waves and comparing it with the known distance in the distribution feeder, it is possible to identify the faulty section and the probable location of the fault. The results from research work suggest that it is possible to locate the faults on the distribution network based on one measurement point where it would be economical for this type of network. The accuracy of the fault location is very accurate (about 200 m or less) depending on the number of waveforms matching performed on the faulted section. Additional research efforts will be undertaken to take into account other power system configurations and the effect of fault resistances to the waveforms generated.

**REFERENCES**

- Ancell, G.B. and N.C. Pahalawaththa, 1994. Maximum likelihood estimation of fault location on transmission lines using travelling waves. *IEEE Trans. Power Delivery*, 9: 680-689.
- Bewley, L.V., 1951. Travelling waves on transmission systems. John Wiley and Sons Inc., New York.
- Bo, Z.Q., G. Weller and M.A. Redfern, 1999. Accurate fault location technique for distribution system using fault-generated high-frequency transient voltage signals. *IEE Proceedings-Generation, Transmission Distribution*, 146: 73-79.
- Crossley, P.A. and P.G. MacLaren, 1983. Distance protection based on travelling waves. *IEEE Trans. Power Apparatus Syst.*, 102: 2971-2983.
- Crossley, P.A., P.F. Gale and M. Aurangzeb, 2001. Fault location using high frequency travelling waves measured at a single location on a transmission line. *Developments in Power System Protection*. Amsterdam, Holland, 9-12: pp: 403-406.
- Elhaffar, A. and M. Lehtonen, 2004. Travelling waves based earth fault location in 400 kv transmission network using single end measurement. *Large Engineering Systems Conference on Power Engineering*. LESCOPE-04., 28-30: 53-56.
- Evrenosoglu, C.Y. and A. Abur, 2005. Travelling wave based fault location for teed circuits. *IEEE Trans. Power Delivery*, 20 (2): 1115-1121.
- Gale, P.F. and B.F. Giannattasio, 1994. Travelling waves get to the point. *Modern Power Systems*, pp: 45-47.
- Glover, J.D. and M. Sarma, 2001. *Power System Analysis and Design*, 3rd Edn. Thomson-Engineering, USA.
- Jie Liang, S. Elangovan and J.B.X. Devotta, 1999. Adaptive travelling wave protection algorithm using two correlation functions. *IEEE Trans. Power Delivery*, 14 (1): 126-131.
- Thomas, D.W.P., C. Christopoulos, Y. Tang, P. Gale and J. Stokoe, 2004. Single ended travelling wave fault location scheme based on wavelet analysis. *Eighth IEE International Conference on Developments in Power System Protection*, 1: 196-199.
- Xiangjun, X., K.K. Li, Liu Zhengyi and Yin Xianggen, 2004. Fault location using traveling wave for power networks. *Industry Applications Conference*. 39th IAS Annual Meeting, 3-7: 2426-2429.